HHS Public Access

Author manuscript

*Nature*. Author manuscript; available in PMC 2019 April 03.

Published in final edited form as:

*Nature*. 2018 November ; 563(7731): 360–364. doi:10.1038/s41586-018-0600-6.

# Antibody and TLR7 Agonist Delay Viral Rebound in SHIV-Infected Monkeys

**Erica N. Borducchi**[#1], **Jinyan Liu**[#1], **Joseph P. Nkolola**[#1], **Anthony M. Cadena**[#1], **Wen-Han Yu**[2], **Stephanie Fischinger**[2], **Thomas Broge**[2], **Peter Abbink**[1], **Noe B. Mercado**[1], **Abishek Chandrashekar**[1], **David Jetton**[1], **Lauren Peter**[1], **Katherine McMahan**[1], **Edward T. Moseley**[1], **Elena Bekerman**[3], **Joseph Hesselgesser**[3], **Wenjun Li**[4], **Mark G. Lewis**[5], **Galit Alter**[2], **Romas Geleziunas**[3], and **Dan H. Barouch**[1,2,**]

[1]Center for Virology and Vaccine Research, Beth Israel Deaconess Medical Center, Harvard Medical School, Boston, MA 02215, USA

[2]Ragon Institute of MGH, MIT, and Harvard, Cambridge, MA 02139, USA

[3]Gilead Sciences, Foster City, CA 94404, USA

[4]University of Massachusetts Medical School, Worcester, MA 01605, USA

[5]Bioqual, Rockville, MD 20852, USA

[#] These authors contributed equally to this work.

## Abstract

The latent viral reservoir is the critical barrier for the development of an HIV-1 cure. Previous studies have shown that potent HIV-1 Env-specific broadly neutralizing antibodies (bNAbs) administered at the time of antiretroviral therapy (ART) discontinuation can exert direct antiviral effects, but whether bNAbs can target the viral reservoir during ART suppression remains unknown. Here we show that the V3 glycan-dependent bNAb PGT121 together with the TLR7 agonist vesatolimod (GS-9620) administered during ART suppression delayed viral rebound following ART discontinuation in SHIV-SF162P3-infected rhesus monkeys that initiated ART during early acute infection. Moreover, the subset of PGT121+GS-9620 treated monkeys that did not show viral rebound following ART discontinuation also did not reveal virus by highly sensitive adoptive transfer and CD8 depletion studies. These data demonstrate the potential of bNAb



[**]Correspondence: Dan H. Barouch (dbarouch@bidmc.harvard.edu).

Author Contributions

D.H.B. and R.G. designed the study. J.H. and R.G. developed the ART formulation and TLR7 agonist. E.B. conducted the cytokine analyses. E.N.B., J.L., J.P.N., A.M.C., P.A., N.B.M., A.C., D.J., and L.P. performed the immunologic and virologic assays. W.H.Y., S.F., T.B., and G.A. led the computational modeling. W.L. led the statistical analysis. M.G.L. led the clinical care of the rhesus monkeys. D.H.B. led the study and wrote the paper with all co-authors.

Author Information

E.B., J.H., and R.G. are employees of Gilead Sciences.

The authors declare no competing financial interests.

**Data availability.** All data generated and analyzed in this study are available from the corresponding author upon reasonable request. Source data for figures from individual animals are available online.

administration together with innate immune stimulation as a possible strategy to target the viral reservoir.

The viral reservoir in latently infected CD4+ T lymphocytes[1–4] is responsible for viral rebound in the vast majority of HIV-1-infected individuals who discontinue ART and represents the key challenge for an HIV-1 cure[5,6]. Multiple HIV-1 cure strategies are currently being pursued. One hypothesis is that activation of reservoir cells may render them more susceptible to immune-mediated destruction[7–9], but direct evidence that this strategy can reduce the viral reservoir *in vivo* has not previously been reported.

Potent HIV-1-specific bNAbs have been shown to reduce viremia in untreated, chronically SHIV-infected rhesus monkeys[10–12] and in HIV-1-infected humans[13,14]. Moreover, bNAbs have been reported to delay viral rebound in HIV-1-infected humans when the antibodies were administered at the time of ART discontinuation[15,16]. These studies demonstrate that bNAbs can exert direct antiviral activity, but whether they can target the viral reservoir during ART suppression remains to be determined. Such a study would require that bNAbs no longer be present at therapeutic levels when ART is discontinued. To explore this concept, we evaluated the capacity of the potent neutralizing antibody PGT121[17,18] and the TLR7 agonist vesatolimod (GS-9620)[19,20] to target the viral reservoir in ART suppressed, SHIV-SF162P3-infected rhesus monkeys.

## Study design

We infected 44 Indian origin rhesus monkeys (*Macaca mulatta*) by the intrarectal route with our rhesus PBMC-derived stock of SHIV-SF162P3[21] and initiated daily subcutaneous administration of a pre-formulated ART cocktail (tenofovir disoproxil fumarate, emtricitabine, dolutegravir)[20] on day 7 of infection (Extended Data Fig. 1). Animals had median plasma viral loads of 4.2–4.3 log RNA copies/ml (range 2.8–5.8 log RNA copies/ml) on day 7 prior to ART initiation (Fig. 1a). Viral loads were balanced among the different groups. Following ART initiation, plasma viremia declined to undetectable levels in most animals by week 3 and in all animals by week 6.

All monkeys were treated with continuous daily ART for 96 weeks and then received one of the following interventions (N=11 animals/group; Fig. 1b, Extended Data Fig. 1): (1) sham, (2) GS-9620 alone, (3) PGT121 alone, or (4) both PGT121+GS-9620. In Groups 2 and 4, animals received 10 oral administrations of 0.15 mg/kg GS-9620 (Gilead Sciences, Foster City, CA) every 2 weeks from weeks 96–114. In Groups 3 and 4, animals received 5 intravenous infusions of 10 mg/kg PGT121 (Catalent Biopharma, Madison, WI) every 2 weeks from weeks 106–114. Thus, in the combination group, animals first received five doses of GS-9620 alone and then received five doses of both PGT121 and GS-9620. ART was continued for 16 weeks after the final PGT121 and GS-9620 administration to allow antibody washout prior to ART discontinuation at week 130. Viral loads remained undetectable in all animals throughout the period of ART suppression with no evidence of viral “blips” through week 130 (Fig. 1b).

## Pharmacodynamics and pharmacokinetics

TLR7 triggering leads to innate immune activation[22,23], and the TLR7 agonist GS-986 resulted in robust CD4+ T cell activation in rhesus monkeys[20]. In the present study, the related TLR7 agonist GS-9620 similarly led to activation of CD4+ T cells, as evidenced by increased CD69 and CD38 expression on CD4+ T cells on the day after each GS-9620 administration (Fig. 2a, Extended Data Fig. 2a; P=0.001 to P=0.03, Mann-Whitney tests). Moreover, GS-9620 led to activation of NK cells (Fig. 2b; P=0.0001 to P=0.01, Mann-Whitney tests) and increased plasma levels of IFN-α, IL-1RA, I-TAC, Eotaxin, MIG, MCP-1, IL-1β, IL-6, IP-10 (Extended Data Fig. 2b).

Serum PGT121 levels were detected after each of the 5 infusions from weeks 106–114 without evidence of induction of anti-drug antibodies (Extended Data Figs. 3, 4a). Following the final PGT121 infusion, PGT121 levels fell rapidly, reflecting the short half-life of this human antibody in monkeys[10]. Serum PGT121 levels declined to undetectable levels (<0.5 μg/ml) in most monkeys by week 120 and in all animals by week 122 (Extended Data Fig. 4a). PGT121 was also undetectable in cell lysates and supernatants from lymph nodes and colorectal biopsies from week 120 (Extended Data Fig. 4b). We previously defined PGT121 levels of 1 μg/ml as the threshold for viral rebound in SHIV-SF162P3-infected rhesus monkeys for PGT121-mediated virologic suppression[10]. Thus, PGT121 levels were below this rebound threshold in peripheral blood and lymphoid and gastrointestinal tissues for 8–10 weeks prior to ART discontinuation at week 130.

## Viral DNA

Viral DNA was largely undetectable in PBMC in all groups of monkeys at week 96 and week 120 using an RT-PCR assay with a sensitivity of 3 DNA copies/$10^6$ CD4+ T cells[20] (Fig. 3a, 3b), presumably as a result of the early initiation and extended duration of suppressive ART. We still detected viral DNA in lymph nodes in the majority of animals at week 96 prior to the interventions, consistent with previous findings in early ART treated, SIVmac251-infected rhesus monkeys[24]. Following the interventions at week 120, we observed similar levels of viral DNA in the sham and GS-9620 alone groups. In contrast, we observed lower levels of viral DNA in lymph nodes in the PGT121+GS-9620 treated monkeys as compared with sham controls at week 120 (Fig. 3b; P=0.004, Mann-Whitney test). We were unable to detect cellular RNA in all groups of monkeys, both at week 96 and at week 120 (data not shown). These data suggest that bNAb administration with innate immune stimulation reduced the viral reservoir in these animals.

## Cellular immune responses

Low levels of Gag-, Env-, and Pol-specific cellular immune responses were observed in all groups of monkeys at week 4, but these responses waned by week 96 and week 120 (Extended Data Fig. 5), presumably reflecting no antigen stimulation during the period of ART suppression. Multi-parameter intracellular cytokine staining at week 120 corroborated these findings and showed minimal to no detectable CD8+ T cell responses in PBMC and lymph nodes in all groups of monkeys (Extended Data Fig. 6a). Lymph node CD8+ T cell

responses and follicular CXCR5+CD8+ T cell responses were also marginal in all groups (Extended Data Fig. 6b). In particular, Gag/Env/Pol-specific CD8+ T cell responses were not higher in the groups that received PGT121 than in the groups that did not receive PGT121 in both PBMC and lymph nodes, suggesting no “vaccinal effect” following antibody administration in this study.

## Viral rebound following ART discontinuation

At week 130, we discontinued ART in all animals and monitored plasma viral loads for 196 days following cessation of ART to assess for viral rebound (Fig. 4a). In the sham control group, 11 of 11 (100%) animals rebounded with high peak viral loads and moderate setpoint viral loads typical of SHIV-SF162P3 infection[20,21]. In the GS-9620 group, 10 of 11 (91%) animals rebounded, and in the PGT121 alone group, 9 of 11 (82%) animals rebounded. In the combination PGT121+GS-9620 group, however, only 6 of 11 (55%) animals rebounded by day 196 following ART discontinuation. The PGT121+GS-9620 treated monkeys that rebounded also showed a 2.6 log reduction of peak viral loads and a 1.5 log reduction of setpoint viral loads as compared with sham controls (Fig. 4b; $P<0.001$, chi-square test comparing total viral load AUC). All animals that rebounded generated robust Gag/Env/Pol-specific cellular immune responses following rebound, which likely contributed to post-rebound virologic control (Extended Data Figure 7a).

The median time to viral rebound in the sham control group and in the GS-9620 alone group was 21 days, whereas the median time to viral rebound in the PGT121+GS-9620 group was 5.3-fold longer at 112 days (Fig. 5a). Overall, the PGT121+GS-9620 group demonstrated significantly delayed viral rebound compared with the sham control group, and the PGT121 alone group had a detectable but more modest effect (Fig. 5a, 5b; $P=0.0001$, Kruskall-Wallis test comparing all groups; $P<0.001$, censored Poisson regression model comparing PGT121+GS-9620 vs sham, PGT121 alone vs sham, and PGT121+GS-9620 vs PGT121 alone). These findings demonstrate that PGT121+GS-9620 was superior to PGT121 alone in delaying viral rebound following ART discontinuation.

The PGT121+GS-9620 treated monkeys that did not rebound by day 196 following ART discontinuation had lower peak pre-ART plasma viral loads at week 1 of infection than the animals that did rebound (Fig. 5c; $P=0.03$, Mann-Whitney test). Moreover, pre-ART viral loads correlated inversely with time to rebound in this group (Fig. 5c; $P=0.03$, $R=-0.62$, Spearman rank-correlation test). Similar trends were observed in the animals that did not rebound in the other groups (Extended Data Fig. 7b). These data suggest that the extent of viral exposure prior to ART initiation was an important determinant of the therapeutic efficacy of PGT121+GS-9620, likely by limiting initial seeding of the viral reservoir.

## Adoptive transfer and CD8 depletion studies

Current viral DNA assays are insufficiently sensitive to predict viral rebound following ART discontinuation, as shown by the rapid rebound in 100% of sham controls in this study (Fig. 4a), despite undetectable viral DNA in PBMC and lymph nodes in a subset of these animals at week 120 (Fig. 3b). These findings are also consistent with clinical observations that have

shown viral rebound despite undetectable levels of viral DNA[25,26]. To assess residual replication-competent virus, we first performed an adoptive transfer study using PBMC and lymph node mononuclear cells (LNMC) from 5 of the 7 animals that did not rebound and for which we had sufficient LNMC cells available from day 140 following ART discontinuation, including 4 of the 5 animals in the PGT121+GS-9620 group and 1 of the 2 animals in the PGT121 alone group. We infused 30 million PBMC and LNMC by intravenous infusion from these 5 animals into naïve rhesus monkeys, as well as from 2 animals in the PGT121+GS-9620 group that showed transient rebound followed by virologic control as positive controls. All animals had undetectable plasma viral RNA on day 140 when PBMC and LNMC were harvested. Adoptive transfer of cells from the 2 animals that rebounded led to efficient infection of the naïve hosts, as evidenced by high plasma viral loads of 6.1–6.8 log RNA copies/ml in recipients by day 14–21 following adoptive transfer (Fig. 6a, red lines). These data show that replication-competent virus persisted in these 2 animals despite post-rebound virologic control. In contrast, adoptive transfer of cells from the 5 animals that did not rebound failed to transfer infection to naïve hosts (Fig. 6a, black lines).

We next depleted CD8+ T cells and NK cells in the animals in the PGT121+GS-9620 group that had undetectable viral loads on day 196 following ART discontinuation. Monkeys received a single intravenous infusion of 50 mg/kg of the anti-CD8α CDR-grafted rhesus IgG1 antibody MT807R1 (provided by Keith Reimann, MassBiologics, Mattapan, MA). Following infusion, all animals showed dramatic CD8 depletion in PBMC (Extended Data Figure 8) as well as in lymph nodes and colorectal biopsies (data not shown). In all the PGT121+GS-9620 treated monkeys that rebounded following ART discontinuation, plasma viral loads spiked to 6.0–6.8 log RNA copies/ml by day 7–14 following CD8 depletion (Fig. 6b, red lines). In contrast, in the 5 PGT121+GS-9620 treated monkeys that did not rebound following ART discontinuation, viral loads remained undetectable following CD8 depletion (Fig. 6b, black lines).

## Mechanistic studies

We developed a computational model that included cellular activation, innate plasma cytokines, and adaptive immune responses to define correlates of delayed viral rebound. A model that included NK cell activation best correlated with delayed viral rebound (Extended Data Fig. 9a; $P=5.31\times10^{-4}$, R=0.50, Spearman rank-correlation test). A similar model involving NK cell activation also correlated with reduced viral loads following ART discontinuation (Extended Data Fig. 9b; $P=3.52\times10^{-6}$, R=0.64, Spearman rank-correlation test). These data suggest that activated NK cells may play a key role in PGT121-mediated elimination of infected CD4+ T cells following GS-9620 activation, consistent with the observed NK cell activation (Fig. 2b).

We finally assessed the ability of PGT121, with or without GS-9620, to kill HIV-1-infected CD4+ T cells *in vitro*. GS-9620 led to activation of NK cells and T cells *in vitro* (Extended Data Fig. 10a), consistent with the in vivo data (Fig. 2, Extended Data Fig. 2). Moreover, the combination of PGT121 and GS-9620 led to optimal killing of HIV-1-infected CD4+ T cells *in vitro* (Extended Data Fig. 10b), consistent with previous studies[19]. Taken together, these data suggest a mechanism by which the TLR7 agonist GS-9620 stimulated innate immunity

and activated multiple immune cell subsets *in vivo*, including infected CD4+ T cells (Fig. 2, Extended Data Fig. 2), which may have rendered them more susceptible to PGT121-mediated recognition, as well as effector cells including NK cells (Fig. 2b, Extended Data Fig. 9), which may have facilitated PGT121-mediated elimination of these infected CD4+ T cells.

## Discussion

In this study, we demonstrate that PGT121 together with the TLR7 agonist vesatolimod (GS-9620) delayed viral rebound following ART discontinuation in acutely treated, SHIV-SF162P3-infected rhesus monkeys. Moreover, 5 of 11 animals that received PGT121+GS-9620 showed no viral rebound for >6 months after ART cessation and also did not reveal virus by highly sensitive adoptive transfer and CD8 depletion studies. This proof-of-concept study suggests that bNAb administration combined with innate immune stimulation may represent a promising strategy to target the viral reservoir.

Our findings extend previous studies that have shown direct antiviral activity of HIV-1-specific bNAbs in SHIV-infected rhesus monkeys[10–12] and in HIV-1-infected humans[13–16]. However, these prior studies did not assess the potential of bNAbs to target the viral reservoir, which would require bNAbs to be administered during ART suppression and no longer be present at therapeutic levels following ART discontinuation. We previously defined a PGT121 level of 1 μg/ml as the threshold for viral rebound in SHIV-SF162P3-infected rhesus monkeys for PGT121-mediated virologic control[10]. In the present study, PGT121 levels were undetectable (<0.5 μg/ml) in peripheral blood, lymph nodes, and colorectal tissue for 8–10 weeks prior to ART discontinuation (Extended Data Fig. 4). These findings suggest that the delayed viral rebound in the PGT121+GS-9620 group was likely due to reservoir targeting rather than just direct antiviral activity.

The 5 animals in the PGT121+GS-9620 group that showed sustained remission for >6 months following ART discontinuation also did not reveal virus following adoptive transfer and CD8 depletion studies (Fig. 6), which are sensitive tests for residual replication-competent virus. It has been shown that viral rebound can occur in humans following extended periods of ART-free remission[25,26]. We therefore cannot exclude the possibility that exceedingly low levels of replication-competent virus may still exist in these animals. Nevertheless, there was a clear difference between the animals that rebounded and those that did not rebound in the adoptive transfer and CD8 depletion studies (Fig. 6).

We hypothesize that the mechanism of the therapeutic efficacy of PGT121+GS-9620 involves activation of multiple cell types by GS-9620 and efficient binding and elimination of virally infected CD4+ T cells by PGT121. GS-9620 activated CD4+ T cells and NK cells, both *in vivo* (Fig. 2, Extended Data Fig. 2) and *in vitro* (Extended Data Fig. 10). We were unable to show explicitly increased HIV-1 *env* transcription in the infected CD4+ T cells following activation, likely due to limited assay sensitivity. Nevertheless, we observed that activated NK cells correlated with delayed viral rebound following ART discontinuation (Extended Data Fig. 9). These studies suggest that GS-9620 may have activated latently infected CD4+ T cells, which likely rendered them more susceptible to PGT121 binding,

and effector cells such as NK cells, which likely facilitated antibody-mediated elimination of these infected CD4+ T cells. A prediction from this proposed mechanism is that longer duration of PGT121+GS-9620 therapy may improve therapeutic efficacy. In the PGT121+GS-9620 treated animals, we did not detect evidence of a "vaccinal effect" involving increased autologous antigen-specific CD8+ T cell responses following bNAb administration (Extended Data Figs. 5, 6), in contrast with a prior study that involved bNAb administration during acute SHIV infection[27].

In summary, our data demonstrate that bNAb administration combined with innate immune stimulation can delay viral rebound following ART discontinuation. This study utilized animals that initiated ART on day 7 of acute infection and received prolonged suppressive ART for 2.5 years. Moreover, the maximum therapeutic effect was observed in animals with the lowest pre-ART viral loads (Fig. 5c). These observations suggest that it will likely be far more difficult to achieve similar results in animals that initiate ART during chronic infection, and the implications for typical HIV-1-infected individuals remain unclear. Nevertheless, our data provide an initial proof-of-concept in primates demonstrating the potential of innate immune activation with immune-based elimination of the viral reservoir as a potential HIV-1 eradication strategy.

## Methods

### Animals and study design.

44 outbred Indian-origin, young adult male and female rhesus monkeys (*Macaca mulatta*) were genotyped, and animals expressing protective MHC class I alleles and susceptible and resistant TRIM5α alleles were distributed among the groups. Each group had 0 *Mamu-A*01*, 1–2 *Mamu-B*17*, and 0–1 *Mamu-B*08* animals. Animals were otherwise randomly allocated to groups. All monkeys were housed at Bioqual, Rockville, MD. Animals were infected with a single 500 $TCID_{50}$ dose of our rhesus PBMC-derived SHIV-SF162P3 challenge stock[21] by the intrarectal route. ART was initiated on day 7. Monkeys were bled up to two times per week for viral load determinations. Monkeys received the following interventions starting at week 96 (N=11/group): (1) sham controls, (2) vesatolimod (GS-9620) alone, (3) PGT121 alone, or (4) both (Extended Data Fig. 1). In Groups 2 and 4, animals received 10 oral administrations of 0.15 mg/kg GS-9620 (Gilead Sciences, Foster City, CA) every 2 weeks from weeks 96–114. In Groups 3 and 4, animals received 5 intravenous infusions of 10 mg/kg PGT121 (Catalent Biopharma, Madison, WI) every 2 weeks from weeks 106–114. Cytokine levels were determined by Luminex assays, and T cell and NK cell activation was assessed by multiparameter flow cytometry. Immunologic and virologic assays were performed blinded. ART was discontinued at week 130. All animal studies comply with all relevant ethical regulations and were approved by the Bioqual Institutional Animal Care and Use Committee (IACUC).

### ART regimen.

The formulated antiretroviral therapy (ART) cocktail contained 5.1 mg/mL tenofovir disoproxil fumarate (TDF), 40 mg/mL emtricitabine (FTC), and 2.5 mg/mL dolutegravir

(DTG) in water containing 15% (v/v) kleptose adjusted to pH 4.2. This ART cocktail was administered once daily at 1 ml/kg body weight via the subcutaneous route.

### Adoptive transfer studies.

For adoptive transfer studies, 30 million LNMC and PBMC from PGT121+GS-9620 or PGT121 treated animals, harvested on day 140 following ART discontinuation, were infused intravenously into healthy, SHIV-uninfected rhesus monkeys. Viral loads were assessed in recipient animals weekly following adoptive transfer.

### CD8 depletion studies.

For CD8 depletion studies, animals received a single intravenous infusion of 50 mg/kg of the anti-CD8α CDR-grafted rhesus IgG1 antibody MT807R1 (Keith Reimann, MassBiologics, Mattapan, MA). CD8 T cell counts and viral loads were assessed weekly following anti-CD8 infusion.

### PGT121 pharmacokinetics.

ImmunoClear ELISA plates (Thermo Scientific) were coated with 100 ng/well clade C (C97ZA.012) gp140 Env protein capture reagent overnight at 4°C. Plates were then washed with PBS–0.05% Tween 20 and blocked for 2 hours at room temperature with Blocker Casein in PBS (Pierce). Standard curve calibrators and diluted serum samples were incubated on the plates for 1 h prior to further washing and subsequent incubation with a mouse PGT121 anti-idiotype (1 μg/mL) monoclonal antibody. Plates were washed again and then incubated with 1:1,000 dilution of rabbit anti-mouse IgG-horseradish peroxidase (Thermo Scientific). Finally, plates were washed and developed for 5 minutes using SureBlue (KPL Laboratories) followed by addition of TMB Stop solution (KPL Laboratories). Plates were read at 450nm on a VersaMax microplate reader (Molecular Devices) using Softmax Pro version 6.5.1 software. The SoftMax Pro software calculated 4-Parameter Logistic (4-PL) curve fits for the standard calibrators and the test samples concentrations were determined by interpolation into the calibration curves.

### PGT121 anti-drug antibody (ADA) assays.

ADA assays were performed using the MesoScale Discovery (MSD) electrochemiluminescence (ECL) platform. In brief, serum samples were diluted in assay buffer and incubated with a master mix containing Sulfo-tagged and biotinylated-tagged PGT121 (at equimolar concentrations of 0.5 μg/mL) overnight at 4°C on an orbital plate shaker. The mixture was then incubated on a streptavidin-functionalized plate and washed, and tripropylamine (TPA) was added and read using an MSD SQ-120 ECL imager. Luminescence was proportional to the amount of ADA. The assay positivity cut-point was defined as the 95th percentile of ECL signal response observed using naïve NHP serum samples.

### Cellular immune assays.

SIV-specific cellular immune responses were assessed by IFN-γ ELISPOT assays and multiparameter ICS assays essentially as described[20]. ICS assays were performed with $10^6$

PBMC or LNMC that were incubated for 6 hours at 37°C with media, 10 pg/ml phorbol myristate acetate (PMA) and 1 μg/ml ionomycin (Sigma-Aldrich), or 1 μg/ml HIV-1 Env, SIV Gag, or SIV Pol peptide pools. Cultures contained monensin (GolgiStop; BD Biosciences), brefeldin A (GolgiPlug; BD Biosciences), and 1 μg/ml of a mAb against human CD49d (clone 9F10). Cells were then stained with predetermined titers of mAbs against CD3 (clone SP34.2; , Alexa 700), CD4 (clone L200; BV786), CD8 (clone SK1; APC H7), CD28 (clone L293, PerCP-Cy5.5), CD95 (clone DX2, BV711), CD20 (clone 2H10, BV570), CCR5 (clone 3A9, PE), BCL6 (clone K112–91, PE-CF594), CXCR5 (clone MU5UBEE, PE-cy7), and PD-1 (clone EH12.2H7, Pacific Blue); and stained intracellularly with IFN-γ (clone B27; BUV395), IL-2 (clone MQ1–17H12; BUV737), TNF-α (clone Mab11; BV650), CD69 (clone FN50, BV510), and Ki67 (clone B56, FITC). IFN-γ backgrounds were <0.05% in PBMC.

### Viral RNA assays.

Viral RNA was isolated from cell-free plasma using a viral RNA extraction kit (Qiagen) and was quantitated essentially as described[24].

### Viral DNA assays.

Levels of proviral DNA were quantitated as previously described[24]. Total cellular DNA was isolated from $5\times10^6$ cells using a QIAamp DNA Blood Mini kit (Qiagen). The absolute quantification of viral DNA in each sample was determined by qPCR using primers specific to a conserved region SIVmac239. All samples were directly compared to a linear virus standard and the simultaneous amplification of a fragment of human GAPDH gene. PCR assays were performed with 100–200 ng sample DNA.

### Computational modeling.

The frequencies of cell populations at week 106 (corresponding to the sixth GS-9620 administration) before and after the intervention were utilized for the computational model. Z-score standardization was performed to have all features mean centered and unit variance scaled. The minimal correlates that best predicted viral rebound (or total viral loads) were identified by using a 2-step model: least absolute shrinkage and selection operator (LASSO) regularization followed by partial least squares regression analysis (PLSR). The LASSO method was used to remove irrelevant features in order to improve the robustness of high-dimensional modeling. Next, PLSR was used to model the covariance relationship between the feature variables (X) and the outcome variables (Y), in the way that PLSR decomposes both X and Y into a hyperplane and maximizes covariance between the hyperplanes. To estimate the minimal correlates that best explain the outcome without overfitting, 5,000 repeated 5-fold nested cross-validation was designed. In each repetition, the dataset was randomly divided into 5 folds, where 80% of the dataset was used for building the model and the remaining holdout set was used to test the model prediction, where the goodness-of-fitness of the model was measured by mean squared error (MSE) between prediction and the outcome. This approach resulted in the generation of a model with the minimal set of the features that generates the best outcome prediction in cross-validation test. In addition, variable importance in projection (VIP), a weighted sum of squares of the PLSR weights that summarized the importance of the features in a PLSR model with multiple components,

was computed. To estimate the statistical significance of the optimized model with the defined correlates, we employed two types of permutation tests (shuffling the outcome label and selecting the randomized correlates) to test the likelihood of obtaining a model prediction accuracy by chance. Each permutation test performed 1,000 times to generate an empirical null distribution, and an exact P-value of the model was computed.

### PGT121-mediated CD4+ T cell killing assay.

Human PBMC were isolated from fresh blood from healthy donors using SepMate PBMC Isolation tubes (Stemcell Technologies) and histopaque (Sigma Aldrich) according to manufacturer's protocol. Using an aliquot of PBMC, CD4+ T cells were isolated for HIV-1 infection using the EasySep Human CD4+ T Cell Isolation Kit (Stemcell Technologies). Remaining PBMC were treated with 1,000 nM GS-9620 or DMSO and cultured at $3.0\times10^6$ cells/mL for 5 days in RPMI 1640 (Sigma Aldrich) media supplemented with L-Glutamine, HEPES, and IL-15 (1 ng/mL) at 37 C. For HIV-1 infection, freshly isolated CD4+ T cells were spinfected for 45min at 1500 RPM with NL4–3 virus (or media for mock infection) and then treated with CD3/CD28 Human T Activator Dynabeads (ThermoFisher Scientific). Infected CD4+ T cells were subsequently cultured for 5 days in R10 and IL-2 (30 units/mL) at 37 C. Cells were counted daily and supplemented with fresh media with IL-2 as needed. On day 5, both sets of cells were counted, washed twice and resuspended in fresh media. HIV-infected CD4+ T cells were incubated with 10 μg/mL of PGT121 for 30min. Co-cultures of infected CD4+ T cells and autologous donor PBMC were then set up at a ratio of 1:10 ($5.0\times10^4$ CD4+ T cells : $5.0\times10^5$ PBMC) and incubated overnight in R10 and IL-2 at 37 C. Following the overnight incubation, cells were stained with Fixable Aqua viability dye (Invitrogen) followed by surface staining with CD4-APC (Invitrogen), CD56-PE-Cy7 (BD), CD3-AF700 (BD), and CD69-BV605 (BD). Cells were fixed and permeabilized with Cytofix/Cytoperm (BD Biosciences) and stained intracellularly with anti-KC57-PE-labeled p24 antibody (Beckman Coulter) in 1x Perm/Wash Buffer (BD Biosciences, 554723). Gating on viable CD3+CD4+p24+ T cells was used to evaluate viral killing with each treatment condition normalized to an uninfected control. Percent killing was normalized to the untreated antibody condition.

### Statistical analyses.

Analysis of virologic and immunologic data was performed using GraphPad Prism v6.03 (GraphPad Software). Comparisons of groups was performed using 2-sided Mann-Whitney tests without Bonferroni adjustments. Correlations were assessed by 2-sided Spearman rank-correlation tests. Analysis of viral rebound was performed using Kruskall-Wallis tests to compare all groups. For group pairwise comparisons, area under the curve (AUC) for total viral RNA following ART discontinuation was compared with chi-square tests, and viral rebound was compared with a censored Poisson regression model. In vitro killing data were analyzed with paired Student's t tests.

## Extended Data

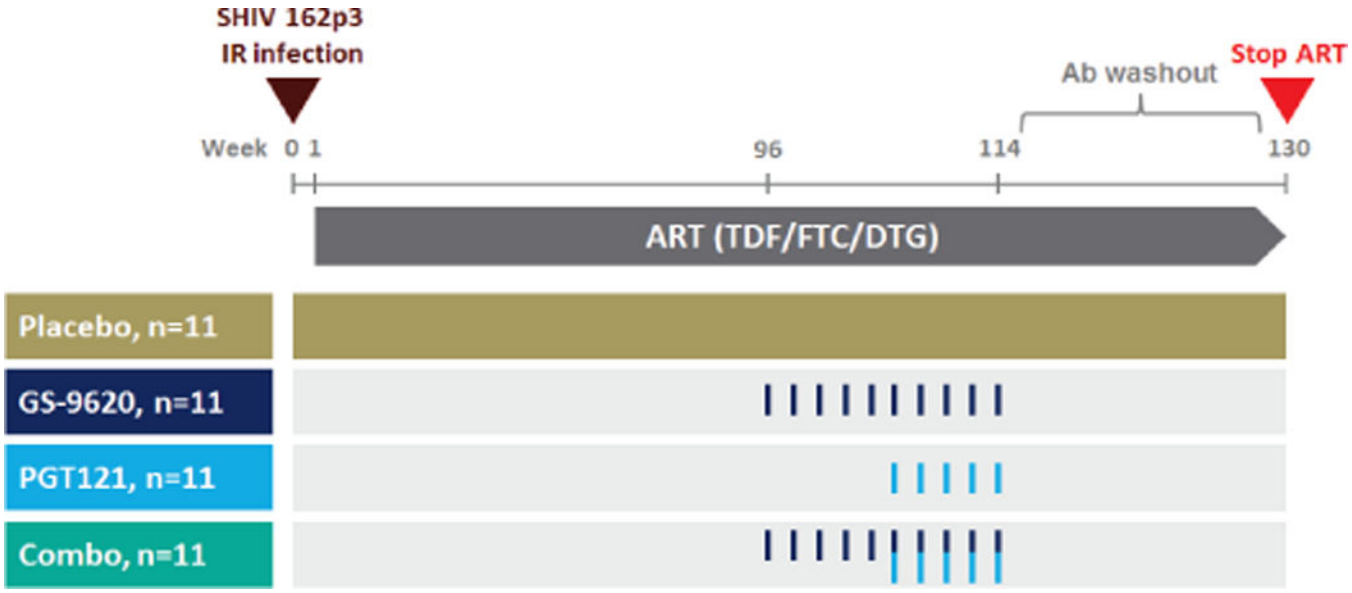


**Extended Data Figure 1. Study design.**

44 rhesus monkeys (N=11 animals/group) were infected with SHIV-SF162P3 at week 0 and initiated ART at week 1 (day 7). GS-9620 administrations and PGT121 infusions are shown from weeks 96–114. ART was discontinued at week 130.

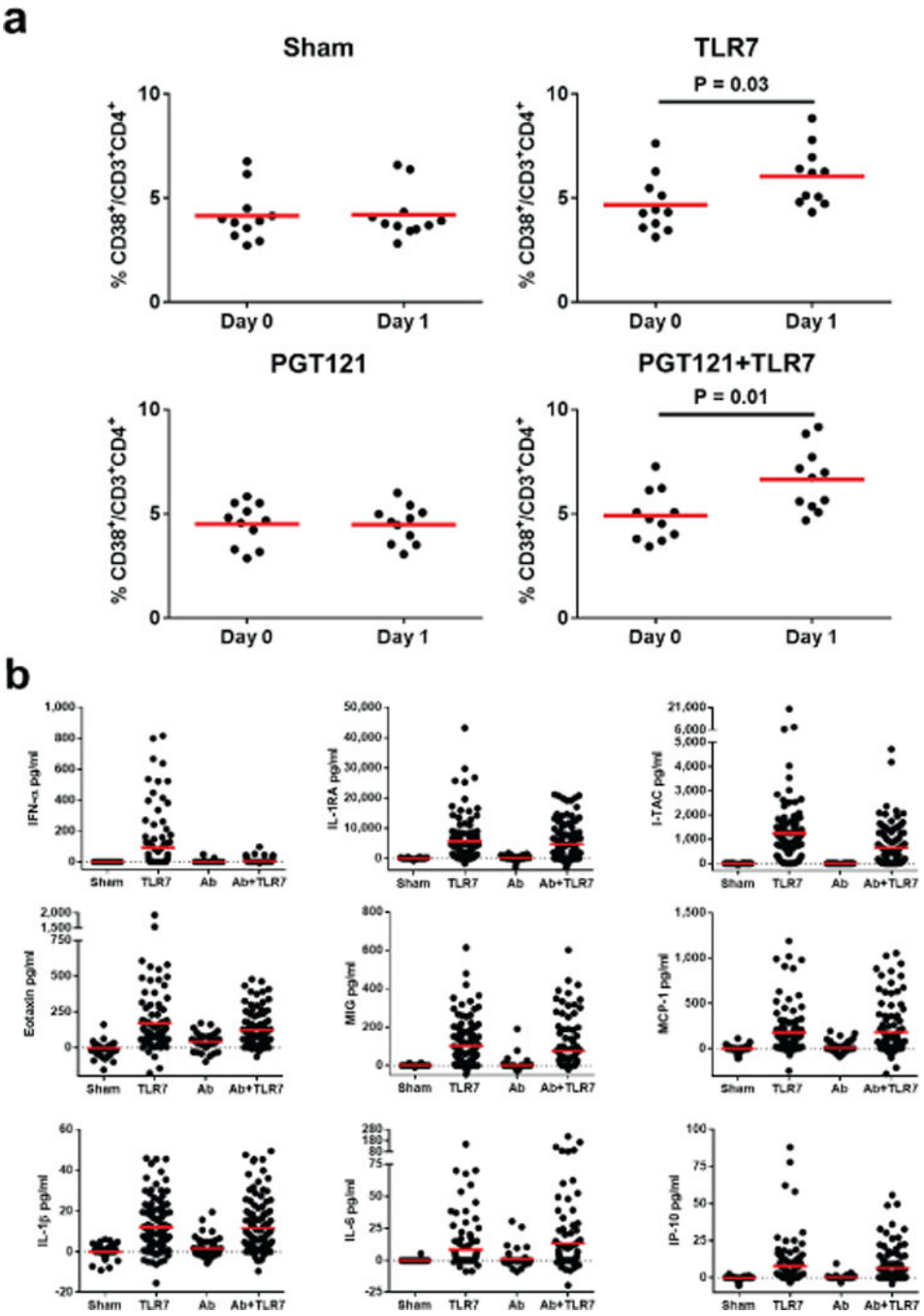


**Extended Data Figure 2. Immune activation following GS-9620 administration and prior to ART discontinuation.**

(**a**) Activation of CD4+ T cells was assessed by CD38 expression on days 0 and 1 following GS-9620 administration, supplementing the data shown in Fig. 2a (N=11 animals/group). Representative data are shown following the fifth GS-9620 dose, which was comparable to the other doses. Red horizontal bars indicate median values. P-values reflect 2-sided Mann-Whitney tests. (**b**) Plasma levels of IFN-α, IL-1RA, I-TAC, Eotaxin, MIG, MCP-1, IL-1β, IL-6, IP-10 are shown on day 1 following GS-9620 administration (N=11 animals/group).

Red bars represent mean values. Combined data from all GS-9620 administrations with pre-dose levels subtracted are shown.

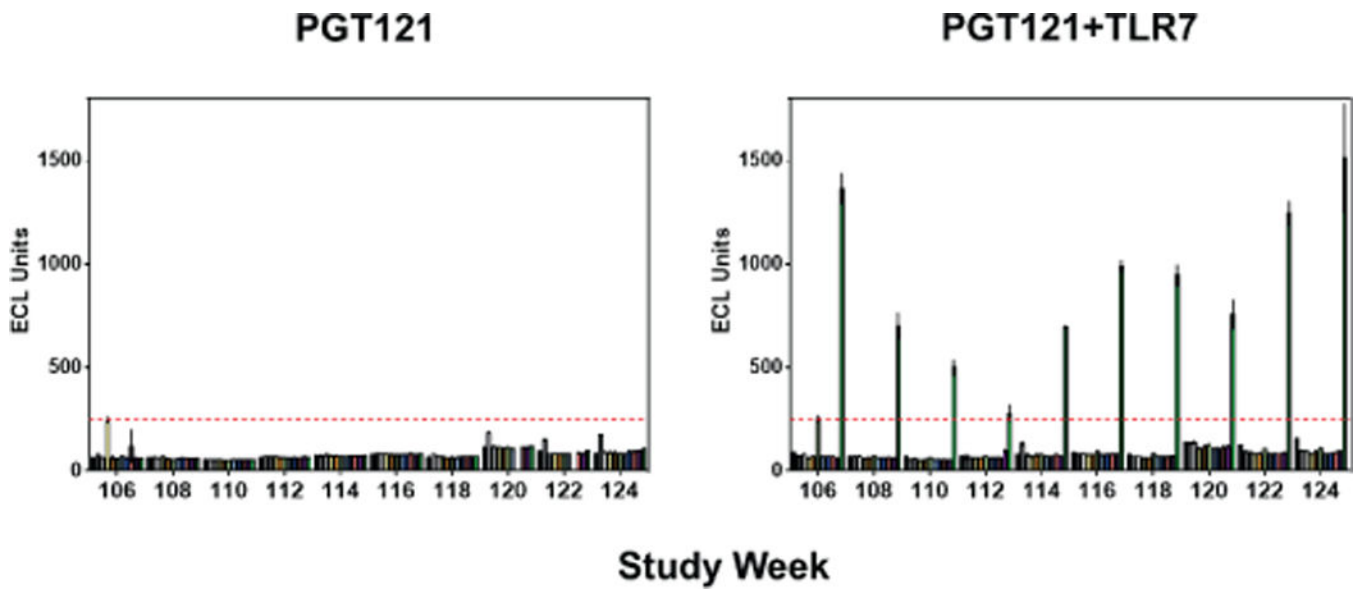


**Extended Data Figure 3. Anti-drug antibody (ADA) assay prior to ART discontinuation.**

ADA responses were assessed in the PGT121+GS-9620 and PGT121 alone groups every 2 weeks from weeks 106–124 an electrochemoluminescence (ECL) assay with an anti-PGT121 idiotypic mAb (N=11 animals/group). No ADA was detected. One animal in the PGT121+GS-9620 group had background reactivity in this assay at week 106 prior to PGT121 exposure (green bars).

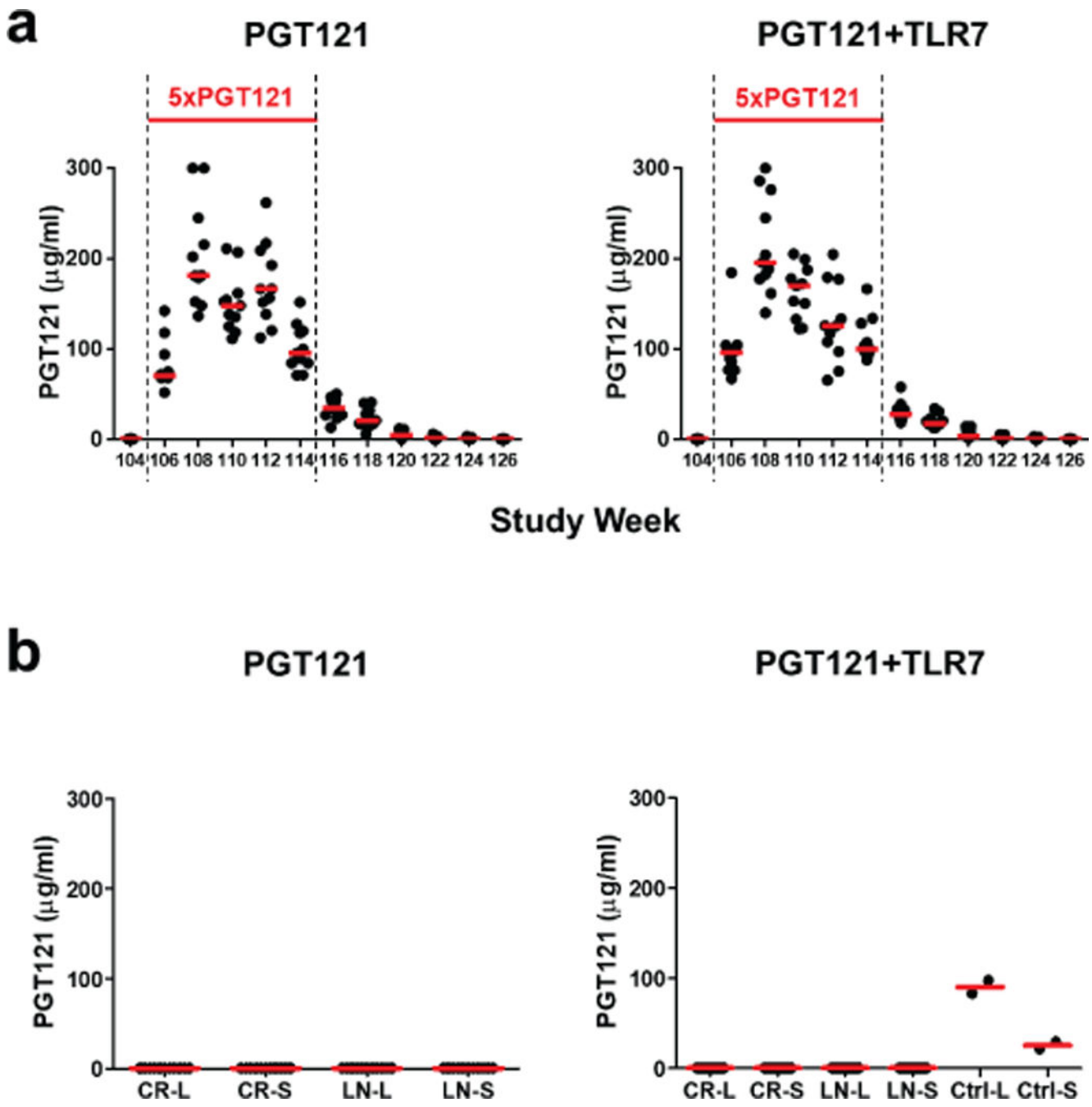


**Extended Data Figure 4. PGT121 pharmacokinetics in serum and tissues prior to ART discontinuation.**

(**a**) Peak serum PGT121 levels are shown (limit of detection 0.5 µg/ml) 1 hour following each of 5 infusions of PGT121 (weeks 106–114) and during the washout period (weeks 114–130) (N=11 animals/group). (**b**) PGT121 levels (limit of detection 0.5 µg/ml) were assessed in cell lysates (L) and initial wash supernatants (S) from $10^6$ lymph node (LN) and colorectal (CR) biopsies from week 120 (N=11 animals/group). Positive controls (Ctrl) included lymph node samples from naïve monkeys spiked with PGT121. Red bars represent median values.

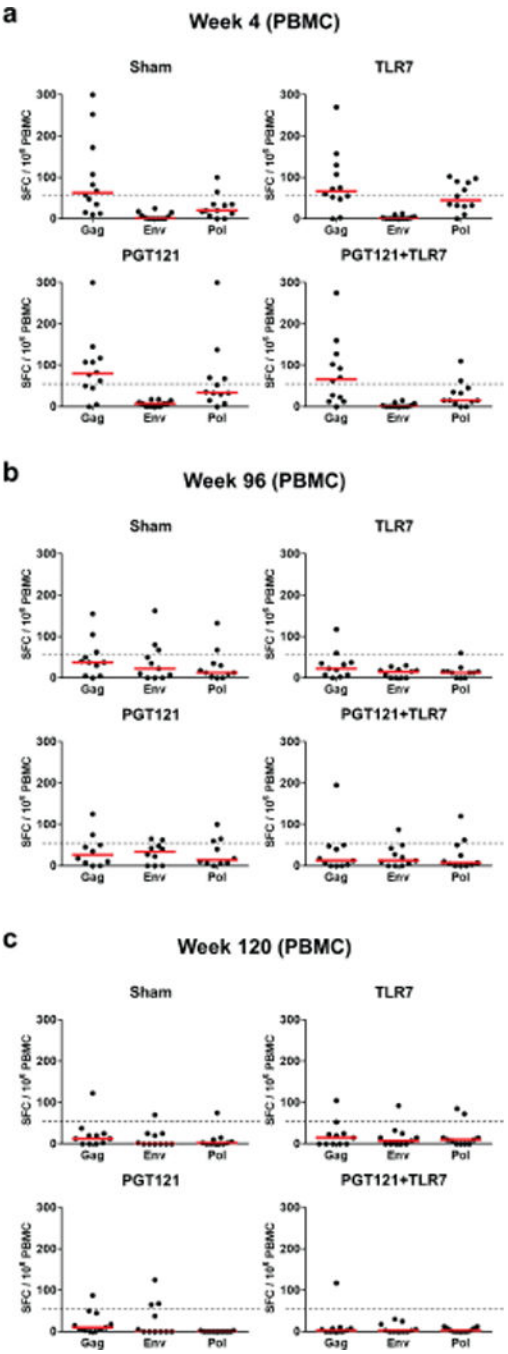


**Extended Data Figure 5. IFN-γ ELISPOT responses prior to ART discontinuation.**

Gag-, Env-, and Pol-specific IFN-γ ELISPOT responses in PBMC are shown at (**a**) week 4, (**b**) week 96, and (**c**) week 120 (N=11 animals/group). Spot-forming cells (SFC) per million PBMC are shown. Red horizontal bars indicate median values. The dotted line represents the assay limit of quantitation (55 SFC/million PBMC).

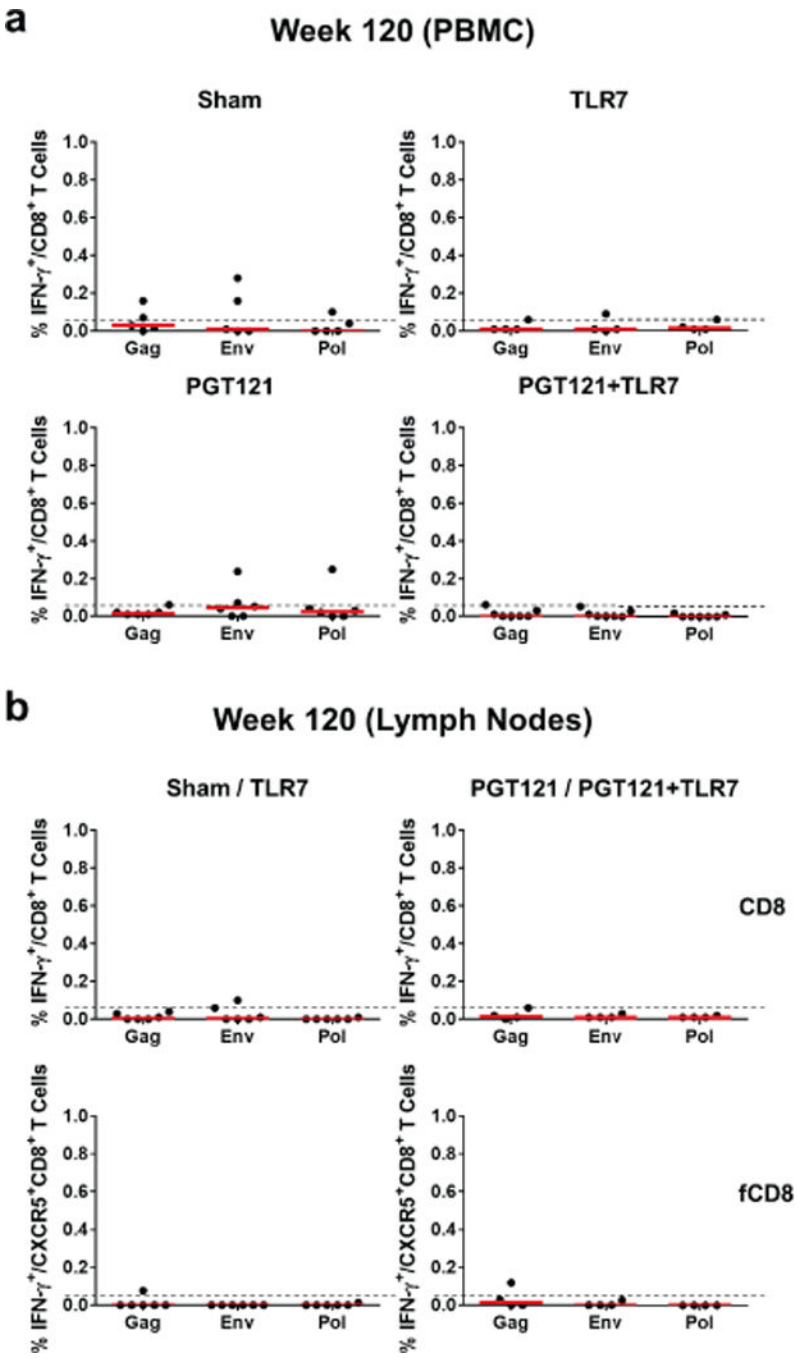


**Extended Data Figure 6. IFN-γ intracellular cytokine staining (ICS) responses prior to ART discontinuation.**

Gag-, Env-, and Pol-specific IFN-γ ICS responses (**a**) in peripheral blood mononuclear cells (PBMC) and (**b**) in lymph node mononuclear cells are shown at week 120 (N=11 animals/group). Percent IFN-γ producing CD8+CD3+ T cells in PBMC and percent IFN-γ producing total CD8+CD3+ T cells (CD8) and follicular CXCR5+CD8+CD3+ T cells (fCD8) in lymph node mononuclear cells are shown. Red horizontal bars indicate median values. The dotted line represents the assay limit of quantitation (0.05% CD8+CD3+ T cells).

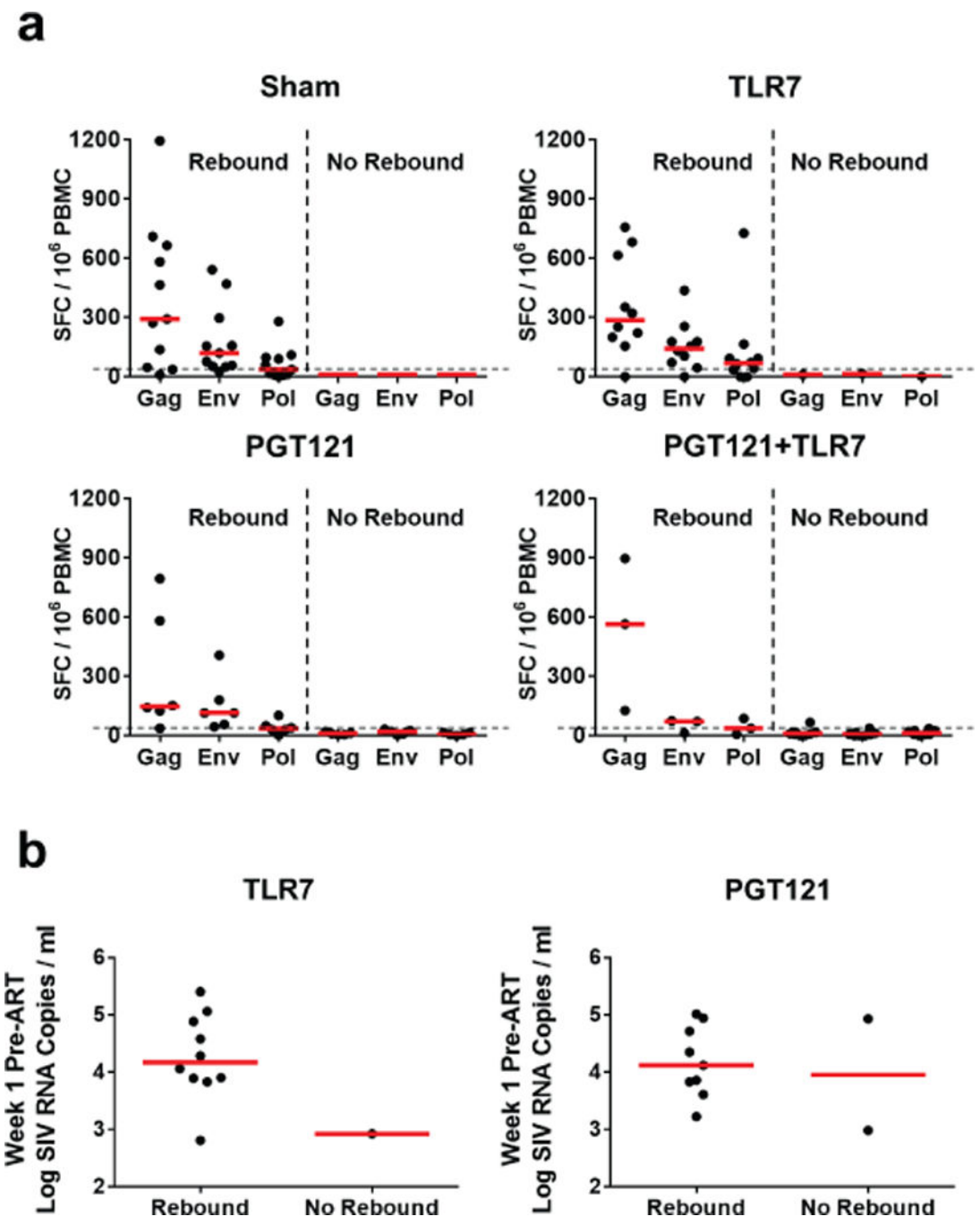


**Extended Data Figure 7. IFN-γ ELISPOT responses following ART discontinuation and trends for viral rebound.**

(**a**) Gag-, Env-, and Pol-specific IFN-γ ELISPOT responses in PBMC are shown at day 140 following ART discontinuation (N=11 animals/group). Spot-forming cells (SFC) per million PBMC are shown. Monkeys in each group that demonstrated viral rebound vs. no rebound are shown separately. Red horizontal bars indicate median values. The dotted line represents the assay limit of quantitation (55 SFC/million PBMC). (**b**) Trends for viral rebound are shown in the GS-9620 alone and the PGT121 alone groups in relation to pre-ART week 1

viral loads, supplementing the data shown in Fig. 5c. Red horizontal bars indicate median values.

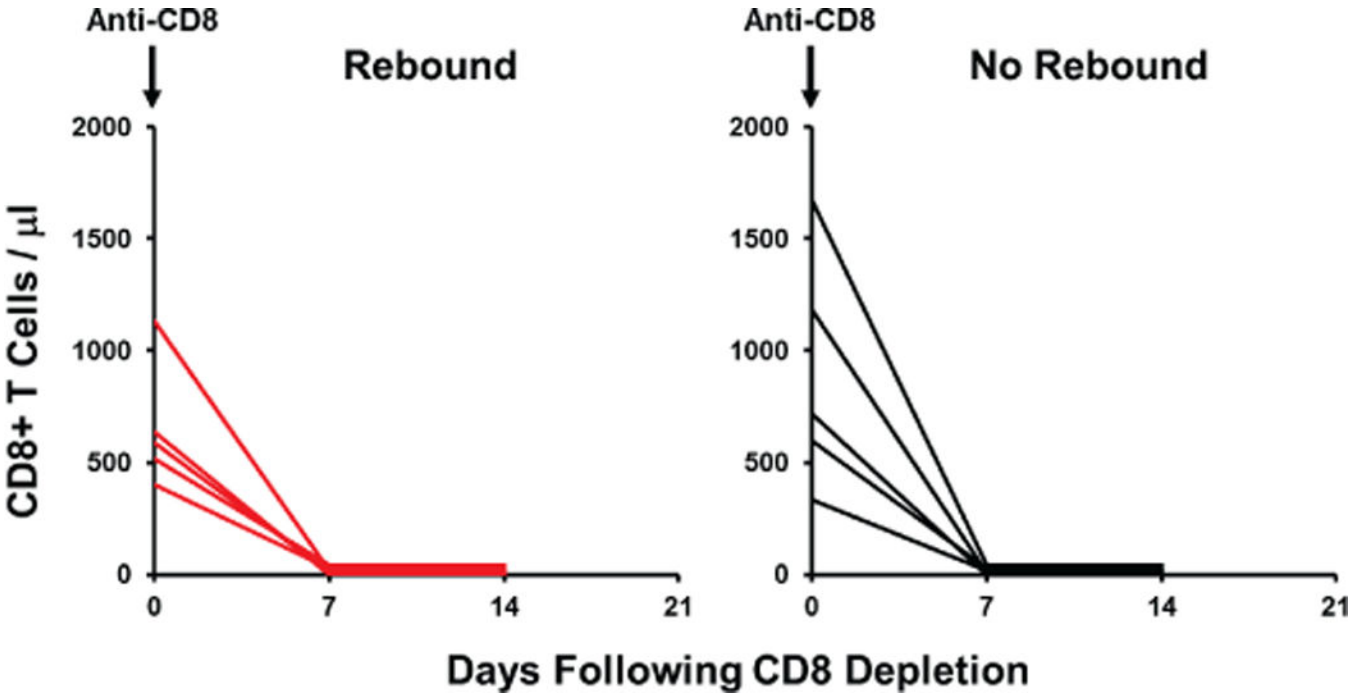


**Extended Data Figure 8. CD8 depletion efficiency.**

CD8+ T cells per µl peripheral blood are shown in PGT121+GS-9620 treated monkeys before and after CD8 depletion in animals that exhibited viral rebound and post-rebound virologic control (N=5, left, red lines) and in animals that exhibited no viral rebound following ART discontinuation (N=5, right, black lines).

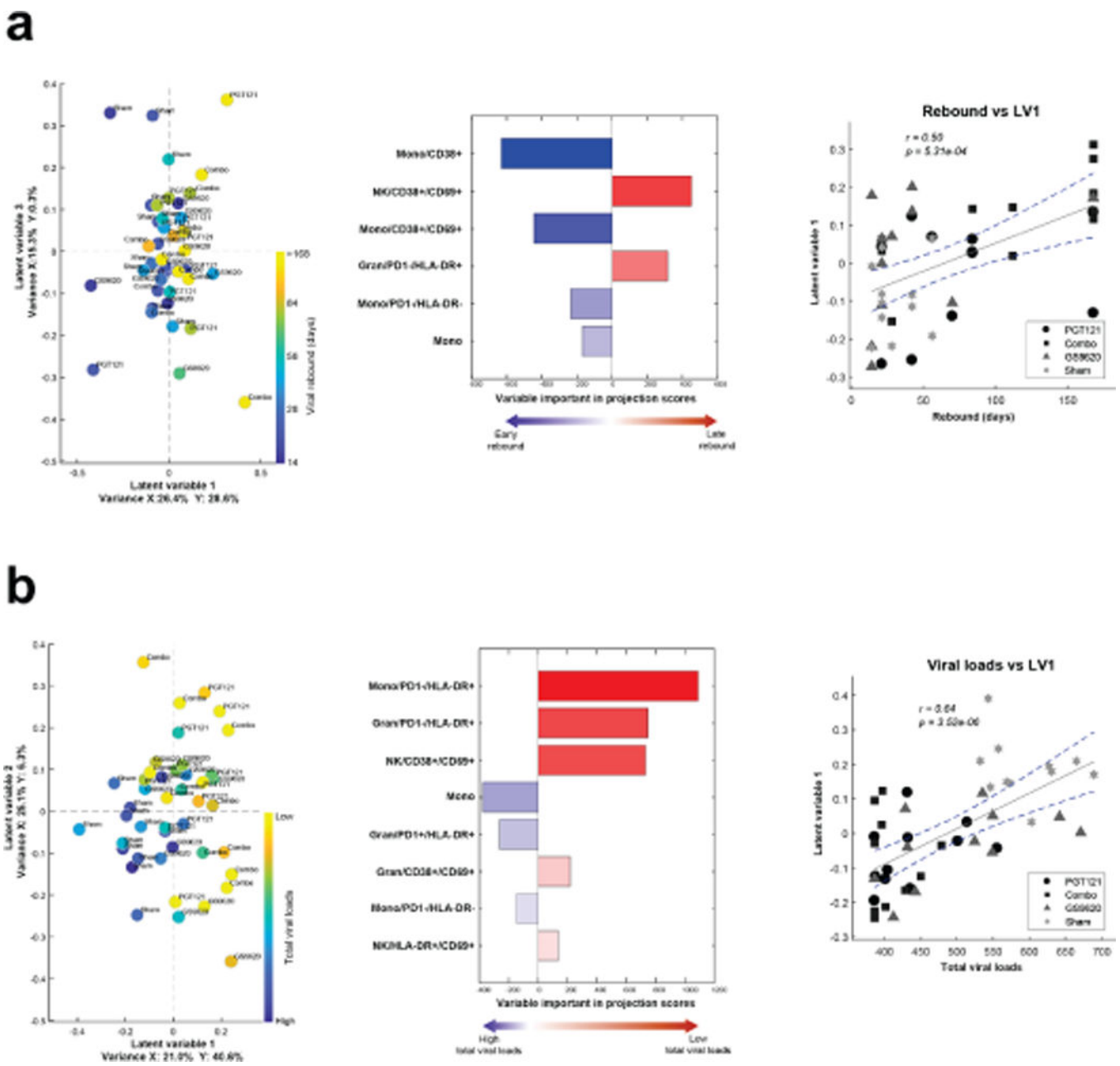


**Extended Data Figure 9. Computational model.**

(**a**) LASSO and PLSR model identifies the parameters that correlate with delayed viral rebound (N=11 animals/group). *Left*, Individual monkeys are showed distributed by latent variables 1 and 3 of the model. Timing of viral rebound is indicated by the color gradient. $R^2$ = 0.176, root mean square error (RMSE) = 0.917, P < 0.001 in 2-sided permutation tests. *Middle*, The contribution of the selected features to model separation is displayed in variable importance in projection (VIP) scores, related to early (blue) or late (red) viral rebound. *Right*, Correlation between viral rebound and latent variable 1. P-value reflects a 2-sided Spearman rank-correlation test. (**b**) LASSO and PLSR model identifies the parameters that correlate with reduced total viral loads (N=11 animals/group). *Left*, Individual monkeys are

showed distributed by latent variables 1 and 2. Total viral loads are indicated by the color gradient. $R^2 = 0.282$, root mean square error (RMSE) = 0.857, $P < 0.001$ in in 2-sided permutation tests. *Middle*, The contribution of the selected features to model separation is displayed in VIP scores, related to high (blue) or low (red) total viral loads. *Right*, Correlation between total viral loads and latent variable 1. P-value reflects a 2-sided Spearman rank-correlation test.

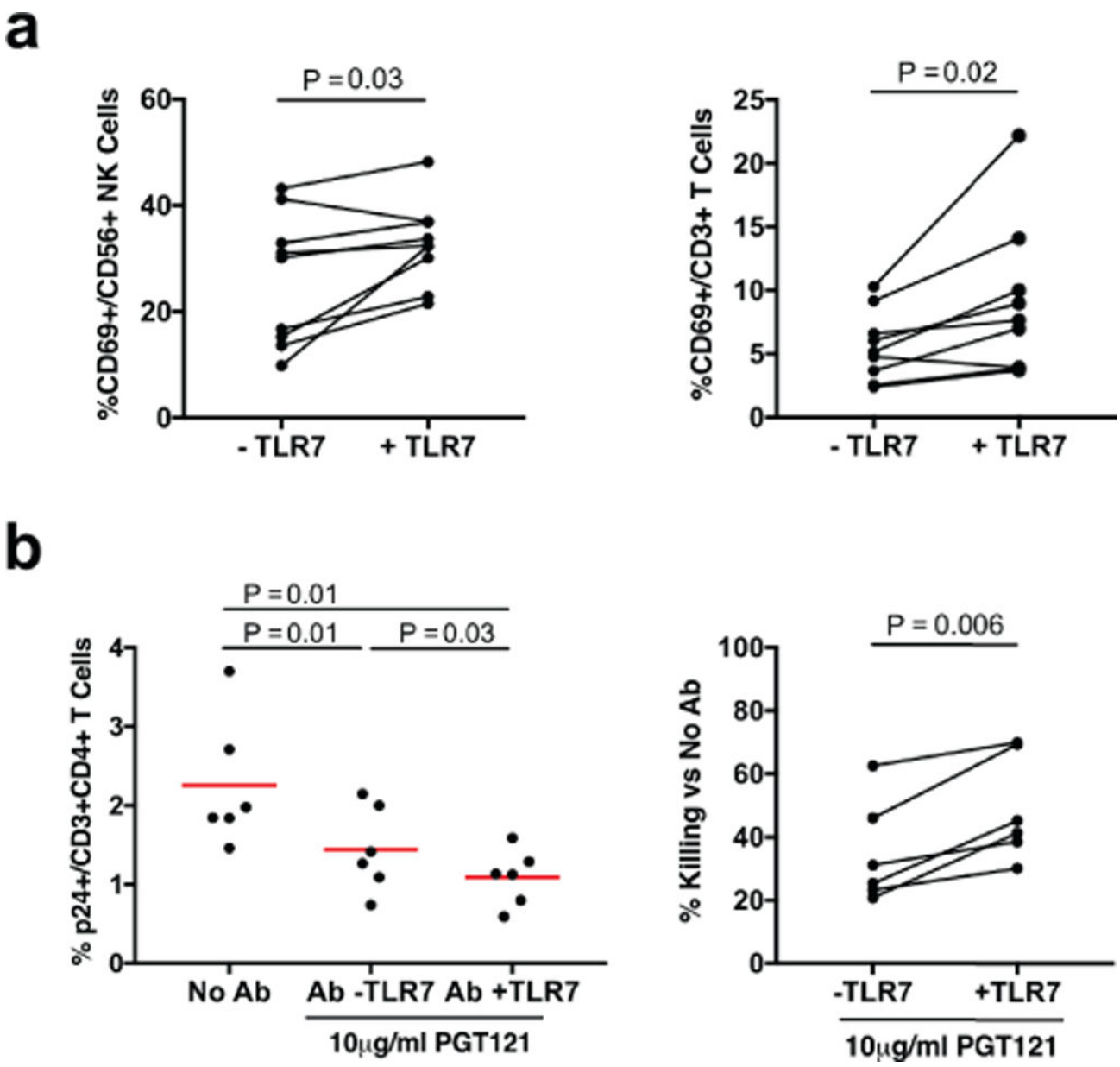


**Extended Data Figure 10. *In vitro* killing studies.**

(**a**) GS-9620 treatment led to CD69 upregulation of CD56+ NK cells and CD3+ T cells *in vitro* following incubation of human PBMC with 1,000 nM GS-9620 for 5 days (N=9). (**b**) GS-9620 treatment augmented PGT121-mediated killing of PGT121 *in vitro*. Percent p24 reduction in CD4+ T cells (N=6) using an antibody-mediated killing assay (see Methods).

Percent killing was calculated as the percent reduction of p24 in CD4+ T cells with PGT121 compared with no PGT121. P-values reflect 2-sided paired Student's t tests.

## Supplementary Material

Refer to Web version on PubMed Central for supplementary material.

## Acknowledgements

We thank Keith Reimann and Alison Hill for generous advice, assistance, and reagents. We acknowledge support from the Bill & Melinda Gates Foundation (OPP1107669), the American Foundation for AIDS Research (109219–58-RGRL), the National Institutes of Health (AI096040, AI124377, AI126603, AI129797, AI128751, OD024917), and the Ragon Institute of MGH, MIT, and Harvard.

## References

1. Finzi D et al. Identification of a reservoir for HIV-1 in patients on highly active antiretroviral therapy. Science 278, 1295–1300 (1997). [PubMed: 9360927]
2. Persaud D, Zhou Y, Siliciano JM & Siliciano RF Latency in human immunodeficiency virus type 1 infection: no easy answers. J Virol 77, 1659–1665 (2003). [PubMed: 12525599]
3. Chun TW et al. Presence of an inducible HIV-1 latent reservoir during highly active antiretroviral therapy. Proc Natl Acad Sci U S A 94, 13193–13197 (1997). [PubMed: 9371822]
4. Ho YC et al. Replication-competent noninduced proviruses in the latent reservoir increase barrier to HIV-1 cure. Cell 155, 540–551, 10.1016/j.cell.2013.09.020 (2013). [PubMed: 24243014]
5. Finzi D et al. Latent infection of CD4+ T cells provides a mechanism for lifelong persistence of HIV-1, even in patients on effective combination therapy. Nat Med 5, 512–517, 10.1038/8394 (1999). [PubMed: 10229227]
6. Chun TW, Davey RT, Jr., Engel D, Lane HC & Fauci AS Re-emergence of HIV after stopping therapy. Nature 401, 874–875, 10.1038/44755 (1999). [PubMed: 10553903]
7. Barouch DH & Deeks SG Immunologic strategies for HIV-1 remission and eradication. Science 345, 169–174, 10.1126/science.1255512 (2014). [PubMed: 25013067]
8. Deeks SG et al. International AIDS Society global scientific strategy: towards an HIV cure 2016. Nat Med, 10.1038/nm.4108 (2016).
9. Shan L et al. Stimulation of HIV-1-specific cytolytic T lymphocytes facilitates elimination of latent viral reservoir after virus reactivation. Immunity 36, 491–501, 10.1016/j.immuni.2012.01.014 (2012). [PubMed: 22406268]
10. Barouch DH et al. Therapeutic efficacy of potent neutralizing HIV-1-specific monoclonal antibodies in SHIV-infected rhesus monkeys. Nature 503, 224–228, 10.1038/nature12744 (2013). [PubMed: 24172905]
11. Shingai M et al. Antibody-mediated immunotherapy of macaques chronically infected with SHIV suppresses viraemia. Nature 503, 277–280, 10.1038/nature12746 (2013). [PubMed: 24172896]
12. Julg B et al. Virological Control by the CD4-Binding Site Antibody N6 in Simian-Human Immunodeficiency Virus-Infected Rhesus Monkeys. J Virol 91, 10.1128/JVI.00498-17 (2017).
13. Caskey M et al. Viraemia suppressed in HIV-1-infected humans by broadly neutralizing antibody 3BNC117. Nature, 10.1038/nature14411 (2015).
14. Caskey M et al. Antibody 10–1074 suppresses viremia in HIV-1-infected individuals. Nat Med 23, 185–191, 10.1038/nm.4268 (2017). [PubMed: 28092665]
15. Scheid JF et al. HIV-1 antibody 3BNC117 suppresses viral rebound in humans during treatment interruption. Nature 535, 556–560, 10.1038/nature18929 (2016). [PubMed: 27338952]
16. Bar KJ et al. Effect of HIV Antibody VRC01 on Viral Rebound after Treatment Interruption. N Engl J Med 375, 2037–2050, 10.1056/NEJMoa1608243 (2016). [PubMed: 27959728]
17. Walker LM et al. Broad neutralization coverage of HIV by multiple highly potent antibodies. Nature 477, 466–470, 10.1038/nature10373 (2011). [PubMed: 21849977]

18. Liu J et al. Antibody-mediated protection against SHIV challenge includes systemic clearance of distal virus. Science, 10.1126/science.aag0491 (2016).
19. Tsai A et al. Toll-Like Receptor 7 Agonist GS-9620 Induces HIV Expression and HIV-Specific Immunity in Cells from HIV-Infected Individuals on Suppressive Antiretroviral Therapy. J Virol 91, 10.1128/JVI.02166-16 (2017).
20. Borducchi EN et al. Ad26/MVA therapeutic vaccination with TLR7 stimulation in SIV-infected rhesus monkeys. Nature 540, 284–287, 10.1038/nature20583 (2016). [PubMed: 27841870]
21. Barouch DH et al. Protective efficacy of a global HIV-1 mosaic vaccine against heterologous SHIV challenges in rhesus monkeys. Cell 155, 531–539, 10.1016/j.cell.2013.09.061 (2013). [PubMed: 24243013]
22. Kawai T et al. Interferon-alpha induction through Toll-like receptors involves a direct interaction of IRF7 with MyD88 and TRAF6. Nat Immunol 5, 1061–1068, 10.1038/ni1118 (2004). [PubMed: 15361868]
23. Hemmi H et al. Small anti-viral compounds activate immune cells via the TLR7 MyD88-dependent signaling pathway. Nat Immunol 3, 196–200, 10.1038/ni758 (2002). [PubMed: 11812998]
24. Whitney JB et al. Rapid seeding of the viral reservoir prior to SIV viraemia in rhesus monkeys. Nature 512, 74–77, 10.1038/nature13594 (2014). [PubMed: 25042999]
25. Henrich TJ et al. Antiretroviral-free HIV-1 remission and viral rebound after allogeneic stem cell transplantation: report of 2 cases. Ann Intern Med 161, 319–327, 10.7326/M14-1027 (2014). [PubMed: 25047577]
26. Persaud D et al. Absence of detectable HIV-1 viremia after treatment cessation in an infant. N Engl J Med 369, 1828–1835, 10.1056/NEJMoa1302976 (2013). [PubMed: 24152233]
27. Nishimura Y et al. Early antibody therapy can induce long-lasting immunity to SHIV. Nature 543, 559–563, 10.1038/nature21435 (2017). [PubMed: 28289286]

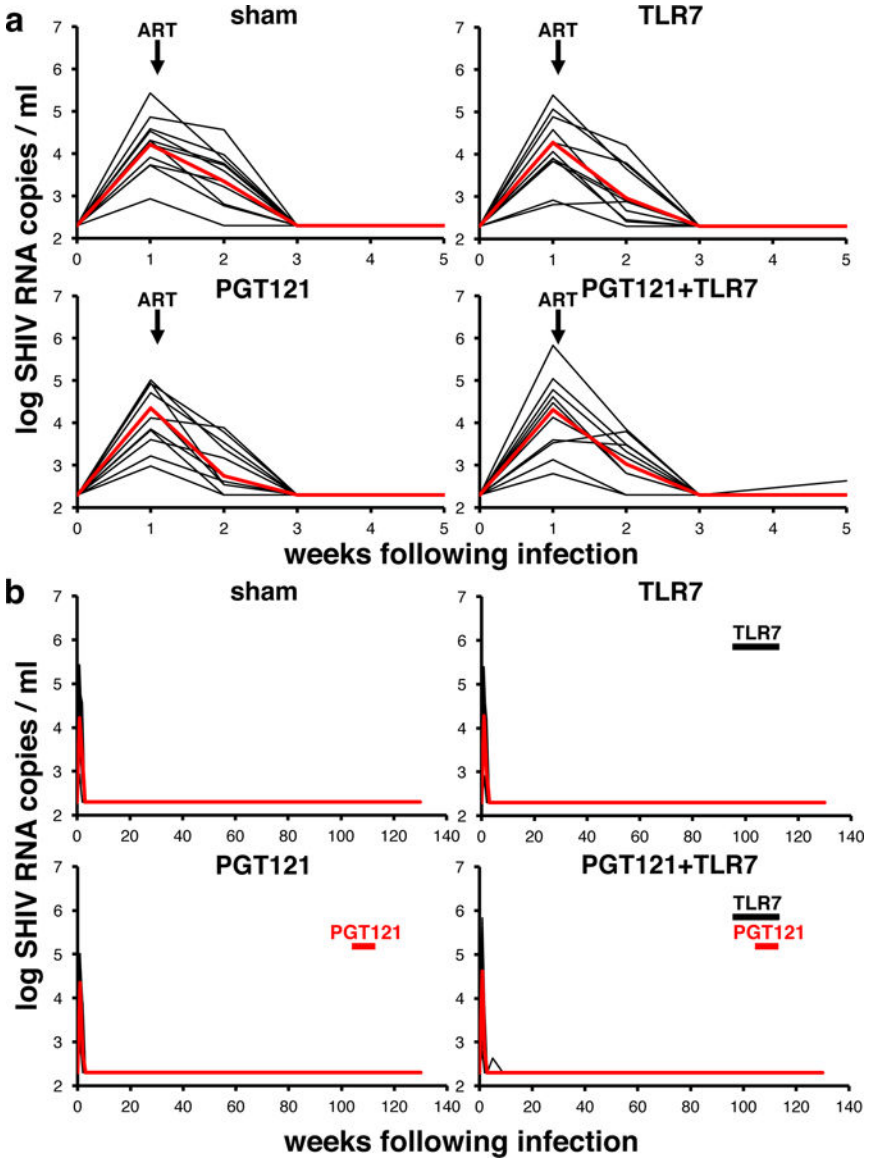


**Figure 1. Plasma viral loads following SHIV-SF162P3 infection and prior to ART discontinuation.**

44 rhesus monkeys were infected with SHIV-SF162P3 at week 0 and initiated ART at week 1 (day 7) (N=11 animals/group). GS-9620 administrations and PGT121 infusions were administered from weeks 96–114. ART was discontinued at week 130. Plasma viral loads are shown for (**a**) weeks 0–5 and (**b**) weeks 0–130. Log SIV RNA copies/ml are shown (limit of detection 2.3 log RNA copies/ml). Red lines indicate median values.

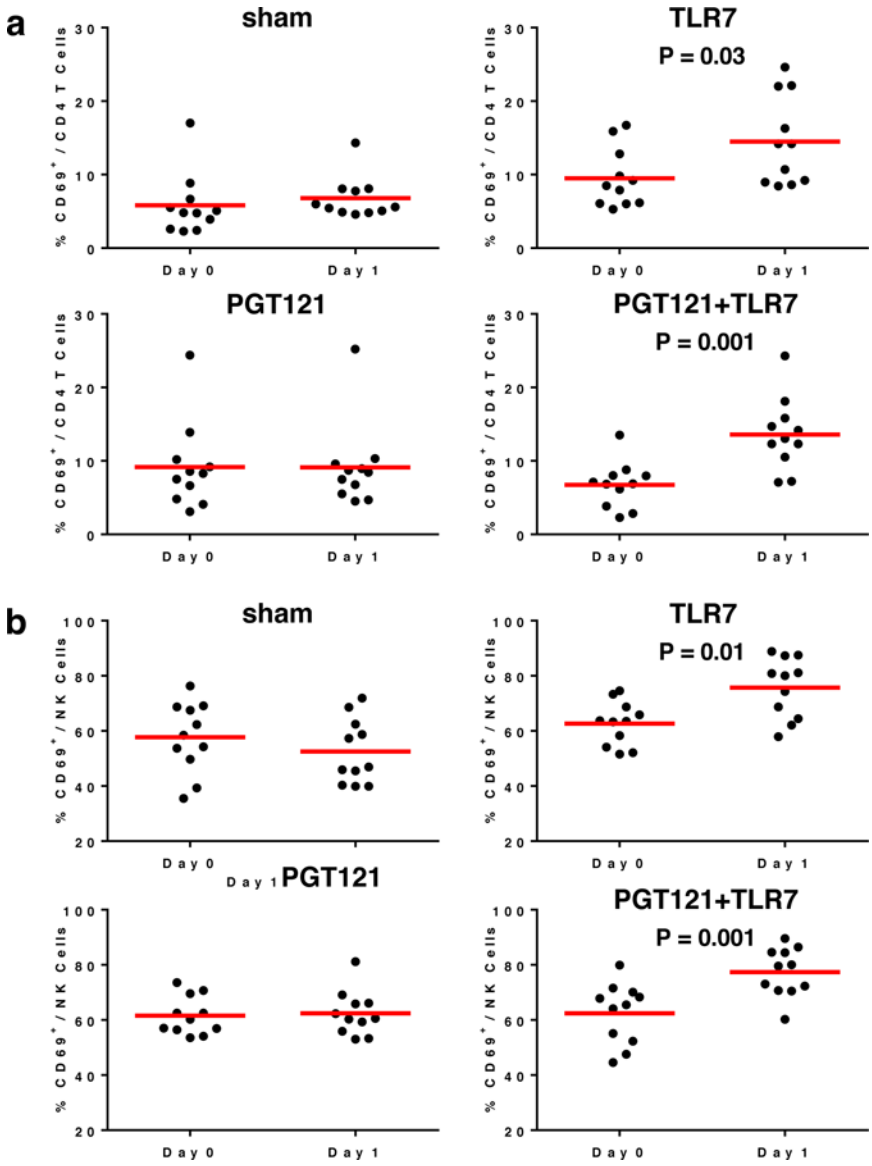


**Figure 2. Cellular immune activation following GS-9620 administration and prior to ART discontinuation.**

Activation of (**a**) CD4+ T cells and (**b**) NK cells in peripheral blood was assessed by CD69 expression on days 0 and 1 following GS-9620 administration (N=11 animals/group). Representative data are shown following the fifth GS-9620 dose, which was comparable to the other doses. Red horizontal bars indicate median values. P-values reflect 2-sided Mann-Whitney tests.

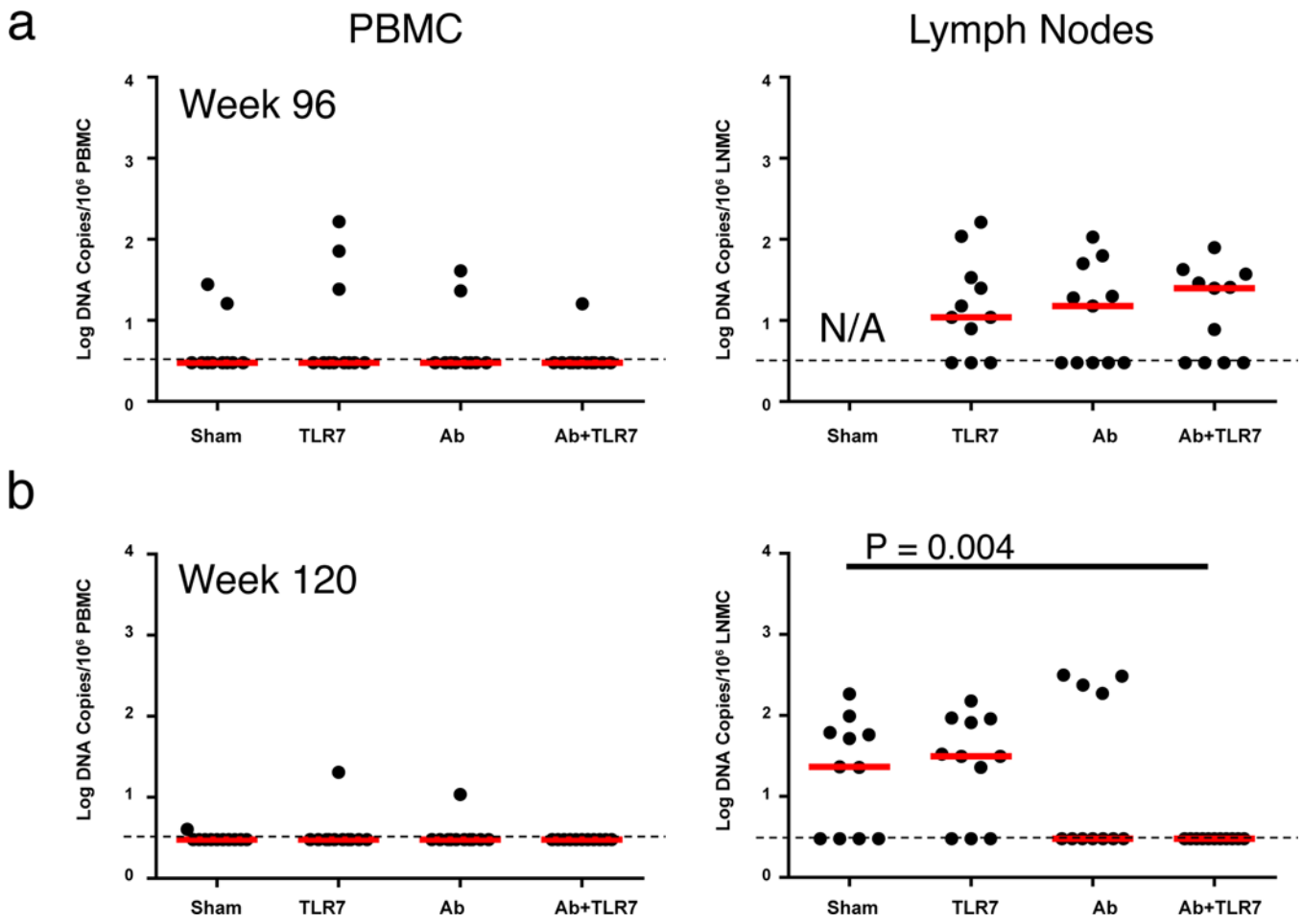


**Figure 3. Viral DNA prior to ART discontinuation.**

Log viral DNA copies/$10^6$ CD4+ T cells are shown (limit of detection 3 DNA copies/$10^6$ cells) in PBMC and lymph nodes prior to the interventions (**a**) at week 96 prior to the interventions and (**b**) at week 120 following the interventions (N=11 animals/group). Red horizontal bars indicate median values. P-values reflect 2-sided Mann-Whitney tests.

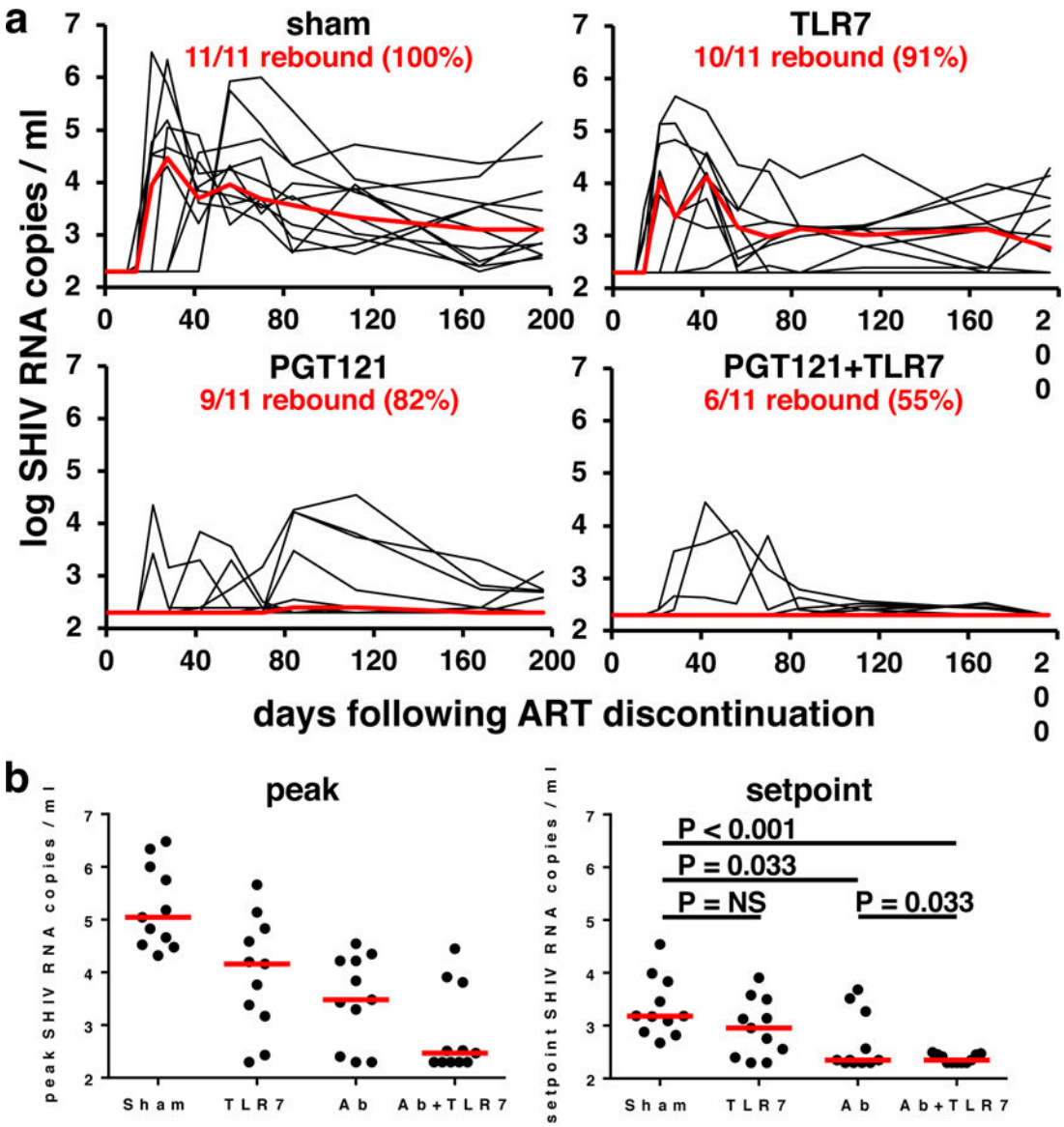


**Figure 4. Viral loads following ART discontinuation.**

(**a**) Plasma viral loads are shown for 196 days following ART discontinuation (N=11 animals/group). Log SIV RNA copies/ml are shown (limit of detection 2.3 log RNA copies/ml). Numbers and percentages of animals that show viral rebound by day 196, defined as any confirmed detectable viral load, are depicted. (**b**) Summary of peak and setpoint viral loads following ART discontinuation (N=11 animals/group). Red lines and horizontal bars indicate median values. P-values reflect chi-square tests of area under the curve (AUC) total viral RNA following ART discontinuation.

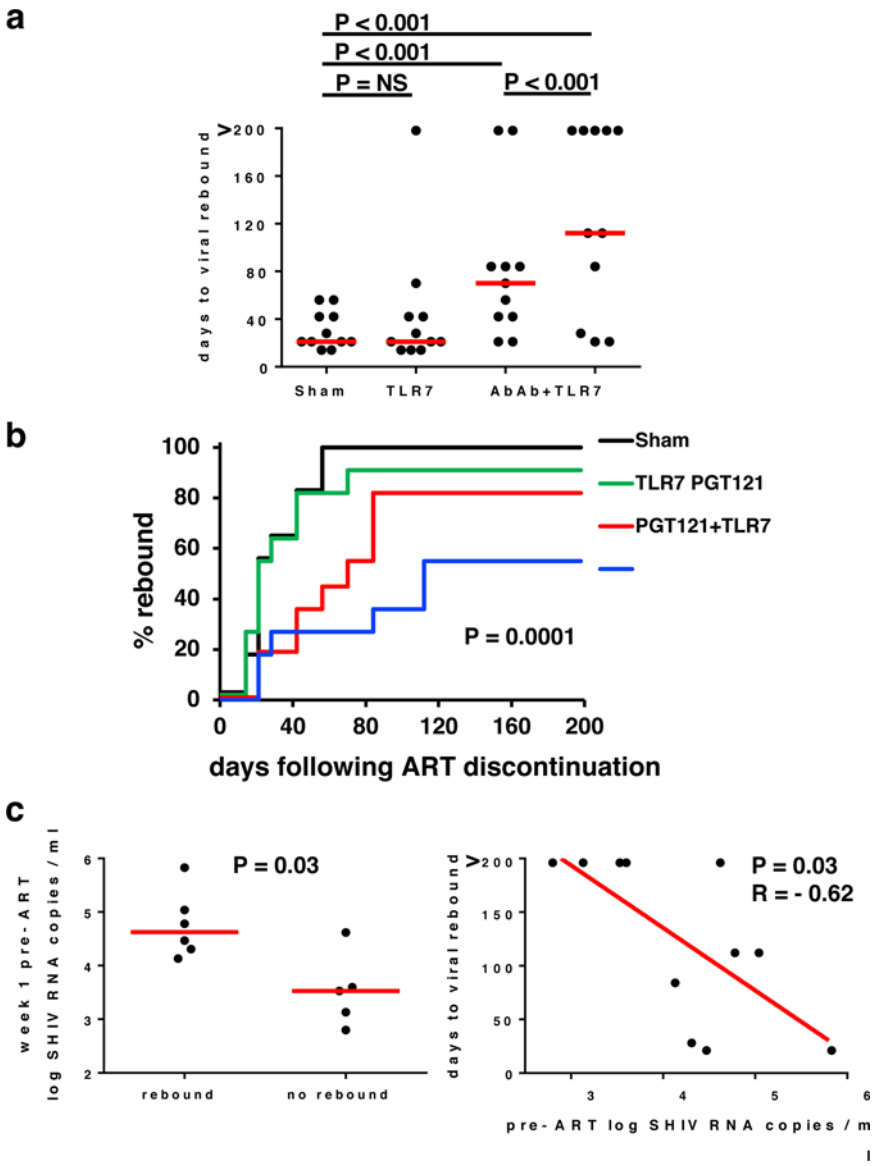


**Figure 5. Analysis and correlations of viral rebound.**

Comparison of time to viral rebound among groups as (**a**) dot plots depicting raw data and (**b**) Kaplan-Meier curves (N=11 animals/group). (**c**) Correlations of viral rebound in PGT121+GS-9620 treated animals with pre-ART week 1 log viral RNA copies/ml (N=11). Red horizontal bars indicate median values. P-values reflect (**a**) a censored Poisson regression model of incidence rate ratios, (**b**) a Kruskall-Wallis test, and (**c**) a 2-sided Spearman rank-correlation test.

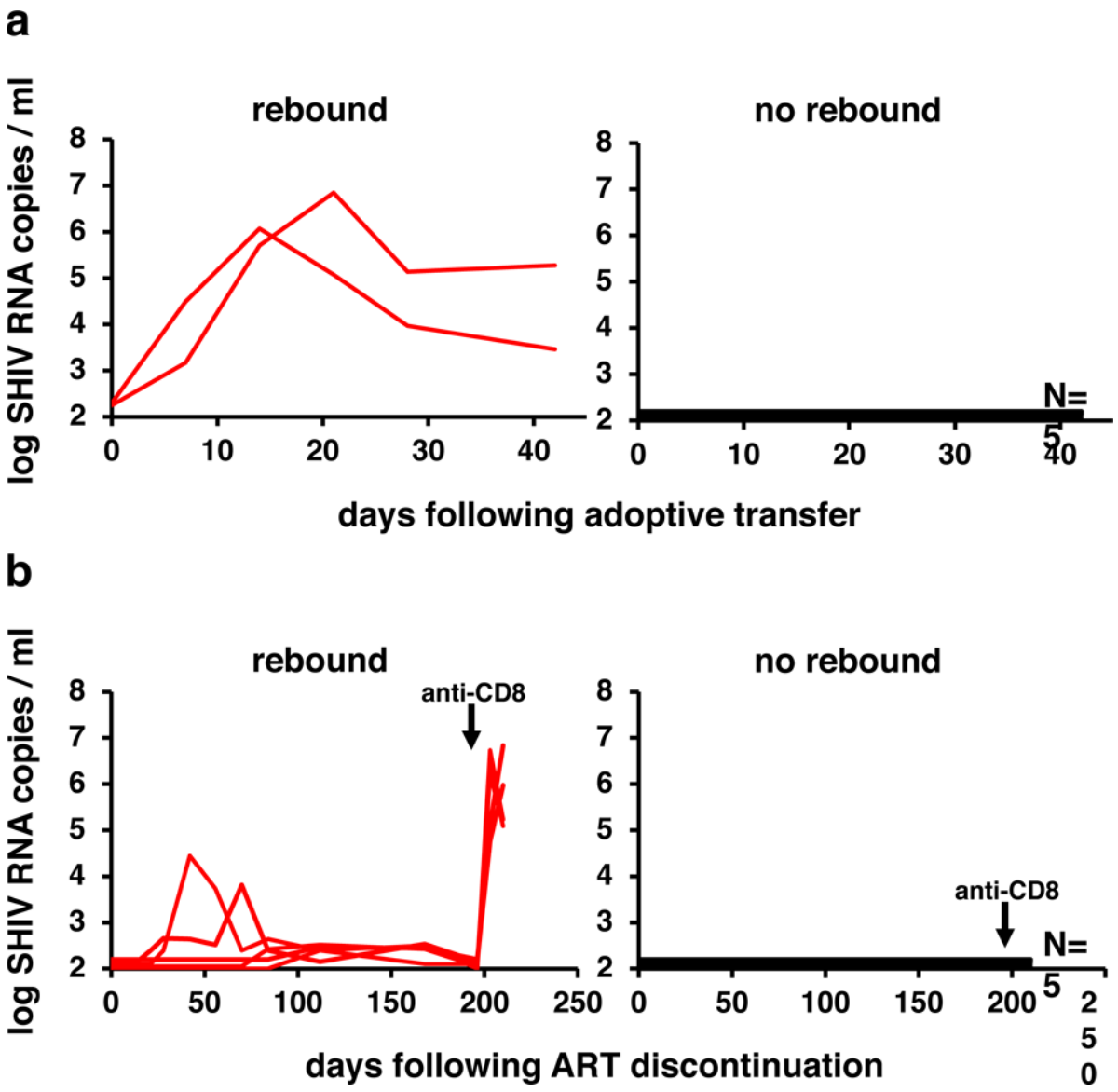


**Figure 6. Adoptive transfer and CD8 depletion studies.**

(**a**) Plasma viral loads are shown in recipient monkeys following adoptive transfer of 30 million PBMC and LNMC from PGT121+GS-9620 treated monkeys that exhibited viral rebound and post-rebound virologic control (N=2, left, red lines) and PGT121+GS-9620 and PGT121 treated monkeys that exhibited no viral rebound following ART discontinuation (N=5, 4 from the PGT121+GS-9620 group and 1 from the PGT121 alone group, right, black lines). (**b**) Plasma viral loads are shown in PGT121+GS-9620 treated monkeys before and after CD8 depletion (see Methods) in animals that exhibited viral rebound and post-rebound virologic control (N=5, left, red lines) and in animals that exhibited no viral rebound following ART discontinuation (N=5, right, black lines). CD8 depletion was performed on day 196 (arrows).